Photoproduction of vector mesons in the soft dipole Pomeron model

E. Martynov,[1,2,*] E. Predazzi,[3,†] and A. Prokudin[3,4,‡]

[1] *Bogolyubov Institute for Theoretical Physics, National Academy of Sciences of Ukraine, 03143 Kiev-143, Metrologicheskaja 14b, Ukraine*

[2] *Institut de Physique Bat B5-a, Université de Liège, Sart Tilman B-4000, Liège, Belgium*

[3] *Dipartimento di Fisica Teorica, Università Degli Studi Di Torino, Via Pietro Giuria 1, 10125 Torino, Italy and Sezione INFN di Torino, Torino, Italy*

[4] *Institute For High Energy Physics, 142281 Protvino, Russia*

(Received 3 October 2002; published 23 April 2003)

Exclusive photoproduction of all vector mesons by real and virtual photons is considered in the soft dipole Pomeron model. It is emphasized that, the Pomeron in this model being a double Regge pole with an intercept equal to 1, we are led to rising cross sections but the unitarity bounds are not violated. It is shown that all available data for $\rho, \omega, \varphi, J/\psi$, and Υ in the region of energies $1.7 \leqslant W \leqslant 250$ GeV and photon virtualities $0 \leqslant Q^2 \leqslant 35$ GeV^2, including the differential cross sections in the region of transfer momenta $0 \leqslant |t| \leqslant 1.6$ GeV^2, are well described by the model.

DOI: 10.1103/PhysRevD.67.074023 PACS number(s): 12.40.Nn, 13.60.Le, 14.40.Gx

I. INTRODUCTION

A new precise measurement of J/ψ exclusive photoproduction by ZEUS [1] opens a new window to our understanding of the process and allows us to give more accurate predictions for future experiments. The key issue of the data set [1] is the diffractive cone shrinkage observed in J/ψ photoproduction which leads us to consider it as a soft rather than pure QCD process so that we can apply the soft dipole Pomeron exchange [2] model.

We are improving the model while not changing its main properties such as the universality for all vector mesons and its applicability in a wide energy region. The structure of the amplitude singularities in the j plane also remains intact but we use a nonlinear Pomeron trajectory in order to describe correctly the behavior of the differential distributions. The use of nonlinear trajectories improves, in fact, the analyticity properties of the scattering amplitude. The secondary Reggeons, however, are for simplicity taken directly with their trajectories as determined from the pure hadronic case. The J/ψ elastic cross section is described as due to the soft Pomeron exchange but without unitarity violation.

We utilize the following picture of the interaction: a photon fluctuates into a quark-antiquark pair and as the lifetime of such a fluctuation is quite long [by the uncertainty principle it grows with the beam energy ν as $2\nu/(Q^2+M_V^2)$ [3]], the proton interacts via Pomeron or secondary Reggeon exchange with this quark-antiquark pair. After the interaction this pair forms a vector meson [4]. The hint is that such an interaction must be very close to that among hadrons and, following the principle of Regge pole theory, that the Pomeron is universal in all hadron-hadron interactions and in all other processes, including deep inelastic scattering, provided we have an appropriate kinematical region for the Regge approach to hold (vacuum quantum number exchange is possible). Thus, if Pomeron exchange is possible, then it has the same properties (the form of singularity, position of such a singularity in the J plane, trajectory, etc.) as in the hadron-hadron interaction. This is true at least for on-shell particles. A real photon ($Q^2=0$) is considered as a hadron (according to the data). For $Q^2 \neq 0$ we assume that no new singularity appears [5]. More precisely, even if we assume a new singularity at $Q^2 \neq 0$, its contribution must be equal to zero for $Q^2=0$. Indeed, the analysis of the data [6] shows that there is no need for such a new contribution.

The basic diagram is depicted in Fig. 1; s and t are the usual Mandelstam variables, and $Q^2=-q^2$ is the virtuality of the photon.

It is well known that the high-energy representation of the scattering amplitude may be expressed as a sum over the the appropriate Regge poles in the complex j plane [7]:

$$A(s,t)_{s\to\infty} \approx \sum_i \eta_i(t)\beta_i(t)(\cos\theta_t)^{\alpha_i(t)}, \tag{1}$$

where $\eta_i(t)$ is the signature factor and θ_t is the scattering angle in the t channel.

In the case of vector meson photoproduction we utilize the variable $z \sim \cos\theta_t$:

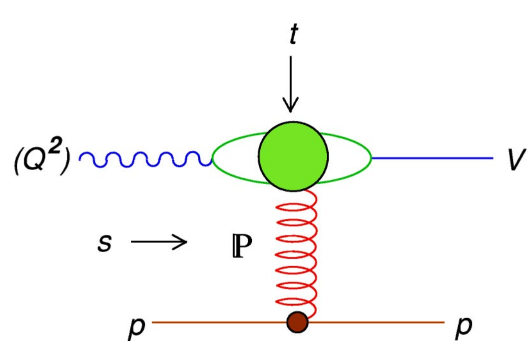

FIG. 1. (Color online) Photoproduction of a vector meson.

*Email address: E.Martynov@guest.ulg.ac.be
†Email address: predazzi@to.infn.it
‡Email address: prokudin@to.infn.it

$$z=\frac{2(W^2-M_p^2)+t+Q^2-M_V^2}{\sqrt{(t+Q^2-M_V^2)^2+4M_V^2Q^2}}, \tag{2}$$

where $W^2=(p+q)^2\equiv s$, M_V is the vector meson mass, and M_p is the proton mass.

Assuming vector meson dominance [8], the relation between the forward cross sections of $\gamma p\to Vp$ and $Vp\to Vp$ is given by

$$\frac{d\sigma}{dt}(t=0)_{\gamma p\to Vp}=\frac{4\pi\alpha}{f_V^2}\frac{d\sigma}{dt}(t=0)_{Vp\to Vp}, \tag{3}$$

where the strength of the vector meson coupling $4\pi/f_V^2$ may be found from the e^+e^- decay width of the vector meson V:

$$\Gamma_{V\to e^+e^-}=\frac{\alpha^2}{3}\frac{4\pi}{f_V^2}m_V. \tag{4}$$

When $V=\rho_0,\omega,\varphi,J/\psi$ the relations of these couplings may be obtained assuming SU(4) flavor symmetry. No attempt is made to extend flavor symmetry to SU(5) so as to incorporate also the Υ coupling. The symmetry is too badly broken for this to make sense. Using the quark content of the mesons, we have

$$\langle Q_j^2\rangle_\rho=\left|\frac{1}{\sqrt{2}}\left(\frac{2}{3}+\frac{1}{3}\right)\right|^2=\frac{1}{2},$$

$$\langle Q_j^2\rangle_\omega=\left|\frac{1}{\sqrt{2}}\left(\frac{2}{3}-\frac{1}{3}\right)\right|^2=\frac{1}{18},$$

$$\langle Q_j^2\rangle_\phi=\left|\frac{1}{3}\right|^2=\frac{1}{9},$$

$$\langle Q_j^2\rangle_{J/\psi}=\left|\frac{2}{3}\right|^2=\frac{4}{9}. \tag{5}$$

Using the property $\Gamma_{V\to e^+e^-}/\langle Q_j^2\rangle\simeq$const we can obtain the following approximate relations:

$$m_\rho/f_\rho^2:m_\omega/f_\omega^2:m_\varphi/f_\varphi^2:m_{J/\psi}/f_{J/\psi}^2=9:1:2:8, \tag{6}$$

which are in fairly good agreement with experimental measurements of decay widths [9].

We take these relations into account by introducing the coefficients N_V (following [10]) and writing the amplitude as $A_{\gamma p\to Vp}=N_CN_VA_{Vp\to Vp}$, where

$$N_C=3,\quad N_\rho=\frac{1}{\sqrt{2}},\quad N_\omega=\frac{1}{3\sqrt{2}},\quad N_\phi=\frac{1}{3},\quad N_{J/\psi}=\frac{2}{3}. \tag{7}$$

The amplitude of the process $Vp\to Vp$ may be written in the following form:

$$A(z,t;M_V^2,\tilde{Q}^2)=\mathbb{P}(z,t;M_V^2,\tilde{Q}^2)+f(z,t;M_V^2,\tilde{Q}^2)+\cdots, \tag{8}$$

where $\tilde{Q}^2=Q^2+M_V^2$.

$\mathbb{P}(z,t;M_V^2,\tilde{Q}^2)$ is the Pomeron contribution for which we use the so called dipole Pomeron which gives a very good description of all hadron-hadron total cross sections [11,12]. Specifically, $\mathbb{P}$ is given by [13]

$$\mathbb{P}(z,t;M_V^2,\tilde{Q}^2)=ig_0(t;M_V^2,\tilde{Q}^2)(-iz)^{\alpha_{\mathbb{P}}(t)-1}+ig_1(t;M_V^2,\tilde{Q}^2)\ln(-iz)(-iz)^{\alpha_{\mathbb{P}}(t)-1}, \tag{9}$$

where the first term is a single j pole contribution and the second [with an additional $\ln(-iz)$ factor] is the contribution of the double j pole.

A similar expression applies to the contribution of the f Reggeon:

$$f(z,t;M_V^2,\tilde{Q}^2)=ig_f(t;M_V^2,\tilde{Q}^2)(-iz)^{\alpha_f(t)-1}. \tag{10}$$

It is important to stress that in this model the intercept of the Pomeron trajectory is equal to 1:

$$\alpha_{\mathbb{P}}(0)=1. \tag{11}$$

Thus the model does not violate the Froissart-Martin bound [14].

For ρ and φ meson photoproduction we write the scattering amplitude as the sum of a Pomeron and an f contribution. According to the Okubo-Zweig rule, the f meson contribution should be suppressed in the production of the φ and J/ψ mesons, but given the present crudeness of the state of the art, we added the f meson contribution in the φ meson case. While we expect the f contribution to J/ψ meson production to be essentially zero, we believe that it is not irrelevant for φ meson production. The f Reggeon can in fact couple with states containing $s(\bar{s})$ quarks due to the production of sea $s(\bar{s})$ quarks or even due to a very small piece of these quarks inside it.

For ω meson photoproduction, we also include π meson exchange (see also the discussion in [15]), which is needed in the low-energy sector, given that we try to describe the data for all energies W. Even though we did not expect it, the model describes the data well down to threshold.

In the integrated elastic cross section

$$\sigma(z,M_V^2,\tilde{Q}^2)_{el}^{\gamma p\to Vp}=4\pi\int_{t_-}^{t_+}dt|A^{\gamma p\to Vp}(z,t;M_V^2,\tilde{Q}^2)|^2, \tag{12}$$

the upper and lower limits

$$2t_\pm = \pm\frac{L_1L_2}{W^2} - (W^2+Q^2-M_V^2-2M_p^2) + \frac{(Q^2+M_p^2)(M_V^2-M_p^2)}{W^2}, \tag{13}$$

$$L_1=\lambda(W^2,-Q^2,M_p^2), \quad L_2=\lambda(W^2,M_V^2,M_p^2), \tag{14}$$

$$\lambda^2(x,y,z)=x^2+y^2+z^2-2xy-2yz-2zx, \tag{15}$$

are determined by the kinematical condition $-1\leqslant\cos\theta_s\leqslant 1$ where θ_s is the scattering angle in the s channel of the process.

The accurate account of the kinematically available t region allows us to describe effectively the threshold behavior of cross sections, so that when $W\to W_{threshold}$ we have $t_-\to t_+$ and the elastic cross section goes to zero. The imaginary part of the amplitude does not vanish at threshold, but it turns out that the kinematical cancellation alone accounts for the threshold behavior. The kinematical character of the threshold behavior of the integrated cross sections was studied long ago [16].

For the Pomeron contribution (9) we use a nonlinear trajectory

$$\alpha_{\mathbb{P}}(t)=1+\gamma(\sqrt{4m_\pi^2}-\sqrt{4m_\pi^2-t}), \tag{16}$$

where m_π is the pion mass. Such a trajectory was utilized for photoproduction amplitudes in [17,18] and its roots are very old [19].

For the f meson contribution for the sake of simplicity we use the standard linear Reggeon trajectory

$$\alpha_{\mathbb{R}}(t)=\alpha_{\mathbb{R}}(0)+\alpha'_{\mathbb{R}}(0)t. \tag{17}$$

In the case of nonzero virtuality of the photon, we have a new variable in play, $Q^2=-q^2$. At the same time, the cross section σ_L is nonzero. According to [4], QCD predicts the following dependence for σ_T, σ_L, and their ratio as Q^2 goes to infinity:

$$\sigma_T\sim\frac{1}{Q^8}[x_{\mathbb{P}}G(x_{\mathbb{P}},\tilde{Q}^2/4)]^2,$$

$$\sigma_L\sim\frac{1}{Q^6}[x_{\mathbb{P}}G(x_{\mathbb{P}},\tilde{Q}^2/4)]^2,$$

$$R\equiv\sigma_L/\sigma_T\sim Q^2/M_V^2,$$

$$\sigma=(\sigma_T+\sigma_L)|_{Q^2\to\infty}\sim\sigma_L, \tag{18}$$

where $x_{\mathbb{P}}G(x_{\mathbb{P}},\tilde{Q}^2/4)$ is the gluon distribution function and $x_{\mathbb{P}}=(Q^2+M_V^2)/(W^2+M_V^2)$ (see, however, [21,22], where another possibility is investigated).

II. THE MODEL

For the Pomeron residues we use the following parametrization:

$$g_i(t;M_V^2,\tilde{Q}^2)=\frac{g_i}{Q_i^2+\tilde{Q}^2}\exp[b_i(t;\tilde{Q}^2)], \quad i=0,1. \tag{19}$$

The slopes are chosen as

$$b_i(t;\tilde{Q}^2)=\left(b_{i0}+\frac{b_{i1}}{1+\tilde{Q}^2/Q_b^2}\right)(\sqrt{4m_\pi^2}-\sqrt{4m_\pi^2-t}), \quad i=0,1, \tag{20}$$

to comply with the previous choice (16) and analyticity requirements [19].

The Reggeon residue is

$$g_{\mathbb{R}}(t;M_V^2,\tilde{Q}^2)=\frac{g_{\mathbb{R}}M_p^2}{(Q_{\mathbb{R}}^2+\tilde{Q}^2)\tilde{Q}^2}\exp[b_{\mathbb{R}}(t;\tilde{Q}^2)], \tag{21}$$

where

$$b_{\mathbb{R}}(t;\tilde{Q}^2)=\frac{b_{\mathbb{R}}}{1+\tilde{Q}^2/Q_b^2}t, \tag{22}$$

g_0, g_1, Q_0^2 (GeV^2), Q_1^2 (GeV^2), $Q_{\mathbb{R}}^2$ (GeV^2), Q_b^2 (GeV^2), b_{00} (GeV^{-1}), b_{01} (GeV^{-1}), b_{10} (GeV^{-1}), b_{11} (GeV^{-1}), and $b_{\mathbb{R}}$ (GeV^{-2}) are adjustable parameters. $\mathbb{R}=f$ for ρ and φ, $\mathbb{R}=f,\pi$ for ω. We use the same slope $b_{\mathbb{R}}$ for f and π Reggeon exchanges.[1]

A. Photoproduction of vector mesons by real photons ($Q^2=0$)

In the fit we use all available data starting from the threshold for each meson. As the new data set of ZEUS [1] provides us with the unique information on both integrated elastic cross section and differential distribution of exclusive J/ψ meson photoproduction, we keep only these data for $Q^2=0$. This allows us to explore the effects of nonlinearity of the Pomeron trajectory and residues. In the region of nonzero Q^2 the combined data of H1 and ZEUS are used.

Different experiments have different normalizations, especially at low energies. This implies that the χ^2 per degree of freedom (DOF) will not be very good, while the overall agreement is quite satisfactory.

The whole set of data is composed of 357 experimental points[2] and, with a grand total of 12 parameters, we find

[1]Of course, the forms of the π Reggeon and of the f Reggeon can be quite different. However, for the sake of economy in the number of parameters, we use the same parametrization.

[2]The data are available at REACTION DATA database http://durpdg.dur.ac.uk/hepdata/reac.html; CROSS SECTION PPDS database http://wwwppds.ihep.su:8001/c1-5A.html

TABLE I. Parameters obtained by fitting ρ_0, ω, φ, and J/ψ photoproduction data.

N	Parameter	Value	Error		Trajectory	$\alpha(0)$	$\alpha'(0)(\mathrm{GeV}^{-2})$
1	γ (GeV^{-1})	0.53853×10^{-1}	0.15666×10^{-1}			Fixed	Fixed
2	g_1	0.10435×10^{-1}	0.17851×10^{-1}	1	f Reggeon	0.8	0.85
3	g_0	-0.32901×10^{-1}	0.49449×10^{-4}	2	π Reggeon	0.0	0.85
4	g_f	0.83371×10^{-1}	0.49503×10^{-3}		Meson	No. of points	χ^2 per point
5	g_π	0.60011	0.21962×10^{-1}	1	$\rho_0(770)$	σ_{el}, 127	1.49
6	Q_0^2 (GeV^2)	0.0	Fixed		$\rho_0(770)$	$d\sigma_{el}/dt$, 24	0.99
7	Q_1^2 (GeV^2)	0.41908	0.23586×10^{-2}	2	$\omega(782)$	σ_{el}, 57	1.65
8	$Q_{\mathbb{R}}^2$ (GeV^2)	0.0	Fixed		$\omega(782)$	$d\sigma_{el}/dt$, 12	0.83
8	Q_b^2 (GeV^2)	3.9724	0.32482	3	$\varphi(1020)$	σ_{el}, 39	0.98
10	b_{10} (GeV^{-1})	2.1251	0.73983×10^{-1}		$\varphi(1020)$	$d\sigma_{el}/dt$, 5	0.61
11	b_{11} (GeV^{-1})	2.5979	0.21451	4	$J/\psi(3096)$	σ_{el}, 29	0.79
12	b_{00} (GeV^{-1})	2.6967	0.24985×10^{-1}		$J/\psi(3096)$	$d\sigma_{el}/dt$, 70	1.92
13	b_{01} (GeV^{-1})	6.7897	0.18717×10^{-1}		All mesons	No. of points	χ^2/DOF
14	$b_{\mathbb{R}}$ (GeV^{-2})	4.5741	0.10509×10^{-2}		$\rho_0,\omega,\varphi,J/\psi$	357	1.49

χ^2/DOF$=1.49$. The main contribution to χ^2 comes from the low-energy region ($W\leqslant4$ GeV); had we started fitting from $W_{min}=4$ GeV, the resulting χ^2/DOF$=0.85$ for the elastic cross sections would be much better and more appropriate for a high-energy model.

In order to get a reliable description and the parameters of the trajectories and residues we use elastic cross sections for each process from threshold up to the highest values of the energy and differential cross sections in the whole t region where data are available: $0\leqslant|t|\leqslant1.6$ GeV^2. The data on the differential cross sections of ρ meson production at $W=71.3$ GeV and φ meson production at $W=13.731$ GeV are not included in the fitting procedure.

The parameters are given in Table I. The errors on the parameters are obtained by MINUIT.

The results are presented in Fig. 2, which also shows the prediction of the model for $\Upsilon(9460)$ photoproduction.

As can be seen, the model describes the vector meson exclusive photoproduction data without the need of a Pomeron contribution with intercept higher than 1. In addition, the rapid rise of the J/ψ cross section at low energies is described as a transition phenomenon, a delay of the onset of the real asymptotic.

Indeed, we can estimate the coefficients a_V in the integrated cross sections at asymptotic energies where the rising component of the Pomeron dominates, $\sigma(z,M_V^2,Q^2=0)_{el}^{\gamma p\to Vp}\approx a_V\ln s$. One can see that independent of the fitted parameters

$$a_{V_1}:a_{V_2}=\left(\frac{N_{V_1}}{N_{V_2}}\right)^2\left(\frac{M_{V_2}}{M_{V_1}}\right)^4$$

and consequently

$$a_\omega:a_\varphi:a_{J/\psi}:a_\rho=0.12:0.68:0.004:1.0.$$

This means that (i) all cross sections, especially $\sigma^{\gamma p\to J/\psi p}$,

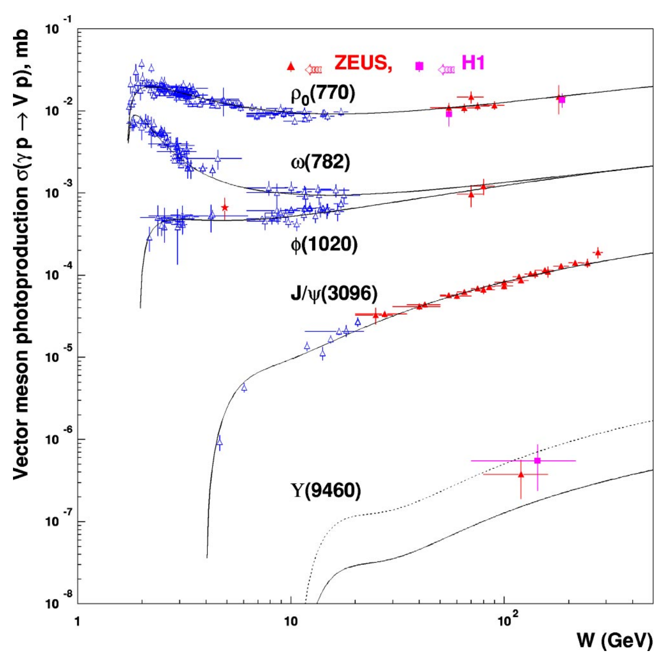

FIG. 2. (Color online) Elastic cross sections for vector meson photoproduction. The solid curve for $\Upsilon(9460)$ production corresponds to $N_\Upsilon=N_\varphi$, the dotted line to $N_\Upsilon=N_{J/\psi}$.

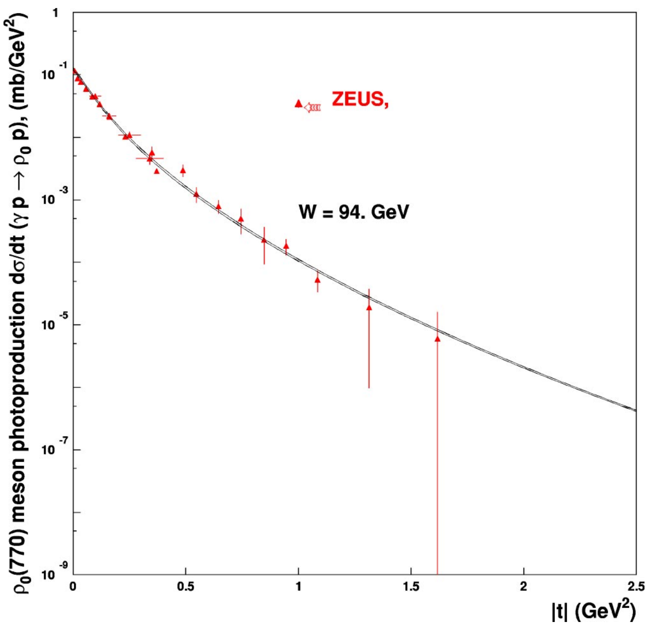

FIG. 3. (Color online) Differential cross section of exclusive ρ_0 meson photoproduction for $W=94$ GeV.

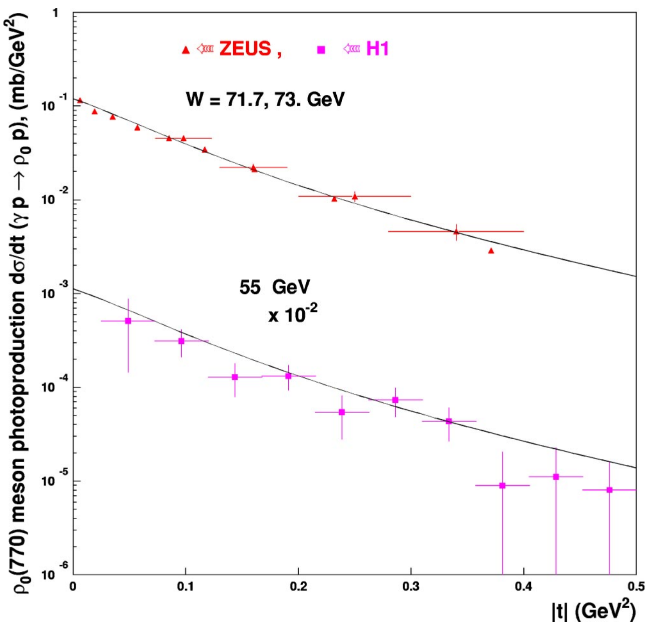

FIG. 4. (Color online) Differential cross section of exclusive ρ_0 meson photoproduction for $W=71.7$, 73, and 55 GeV. The data and curves for $W=55$ GeV are scaled by a factor of 10^{-2}.

rise more slowly than $\sigma^{\gamma p\to\rho p}$ and (ii) $\sigma^{\gamma p\to\varphi p}$ will rise at higher energies faster than $\sigma^{\gamma p\to\omega p}$.

Thus we can conclude that the available experimental data are still rather far from being asymptotic. In the dipole Pomeron model a steep rise of the J/ψ cross section is a temporary phenomenon. If the experiment at higher energies keeps showing a steep growth of the J/ψ integrated elastic cross section, this will imply that the soft dipole Pomeron model, at least the present one, is not applicable to heavy vector meson production.

Had one assumed SU(5) flavor symmetry for the $\Upsilon(9460)$, we would have found $\langle Q_j^2\rangle_\Upsilon=1/9$ and thus $N_\Upsilon=N_\varphi$. This relation leads to underestimating the Υ photoproduction cross section (see the solid line in Fig. 2). Phenomenologically we find that $N_\Upsilon=N_{J/\psi}$ gives a better description of the data on $\Upsilon(9460)$ production (dotted line), but perhaps an intermediate value would be more appropriate.

B. Differential cross section of vector meson exclusive production

The differential cross section is given by

$$\frac{d\sigma}{dt}=4\pi|A(z,t;\tilde{Q}^2,M_V^2)|^2. \tag{23}$$

Using the amplitude from the previous section this quantity is now calculated and the comparison with the data is presented in Figs. 3–8.

Given the universality of our approach we conclude that extracting the Pomeron trajectory from the experimental data as proposed in [20] and [1] using the data depicted in Fig. 5 cannot be regarded as a valid argument to support either the hard Pomeron contribution or the Balitskiĭ-Fadin-Kuraev-Lipatov (BFKL) Pomeron.

Exploring the nonlinearity of the Pomeron trajectory (16) and slopes (19), we have tried adding either a linear term or a heavier threshold; both give negligibly small effects. Thus we conclude that new ZEUS data on $d\sigma_{J/\psi}/dt$ (see, for example, Fig. 6) are a strong support in favor of the nonlinear Pomeron trajectory.

C. Photoproduction of vector mesons by virtual photons ($Q^2>0$)

In Eqs. (19) and (21) the Q^2 dependence ($\tilde{Q}^2=Q^2+M_V^2$) is completely fixed up to an *a priori* arbitrary dimensionless function $f(Q^2)$ such that $f(0)=1$. Thus, we may introduce a new factor that differentiates virtual from real photoproduction:

$$f(Q^2)=\left(\frac{M_V^2}{\tilde{Q}^2}\right)^n. \tag{24}$$

Accordingly, in the case $Q^2\neq 0$ we use the following parametrizations for Pomeron couplings [compare with Eq. (19)]:

$$\hat{g}_i(t;\tilde{Q}^2,M_V^2)=f(Q^2)g_i(t;\tilde{Q}^2,M_V^2),\quad i=0,1, \tag{25}$$

where, for the sake of completeness, we will examine three different choices for the asymptotic Q^2 behavior of the Pomeron residue:

Choice I:

$$n=1,\quad \sigma_T(Q^2\to\infty)\sim\frac{1}{Q^8}; \tag{26}$$

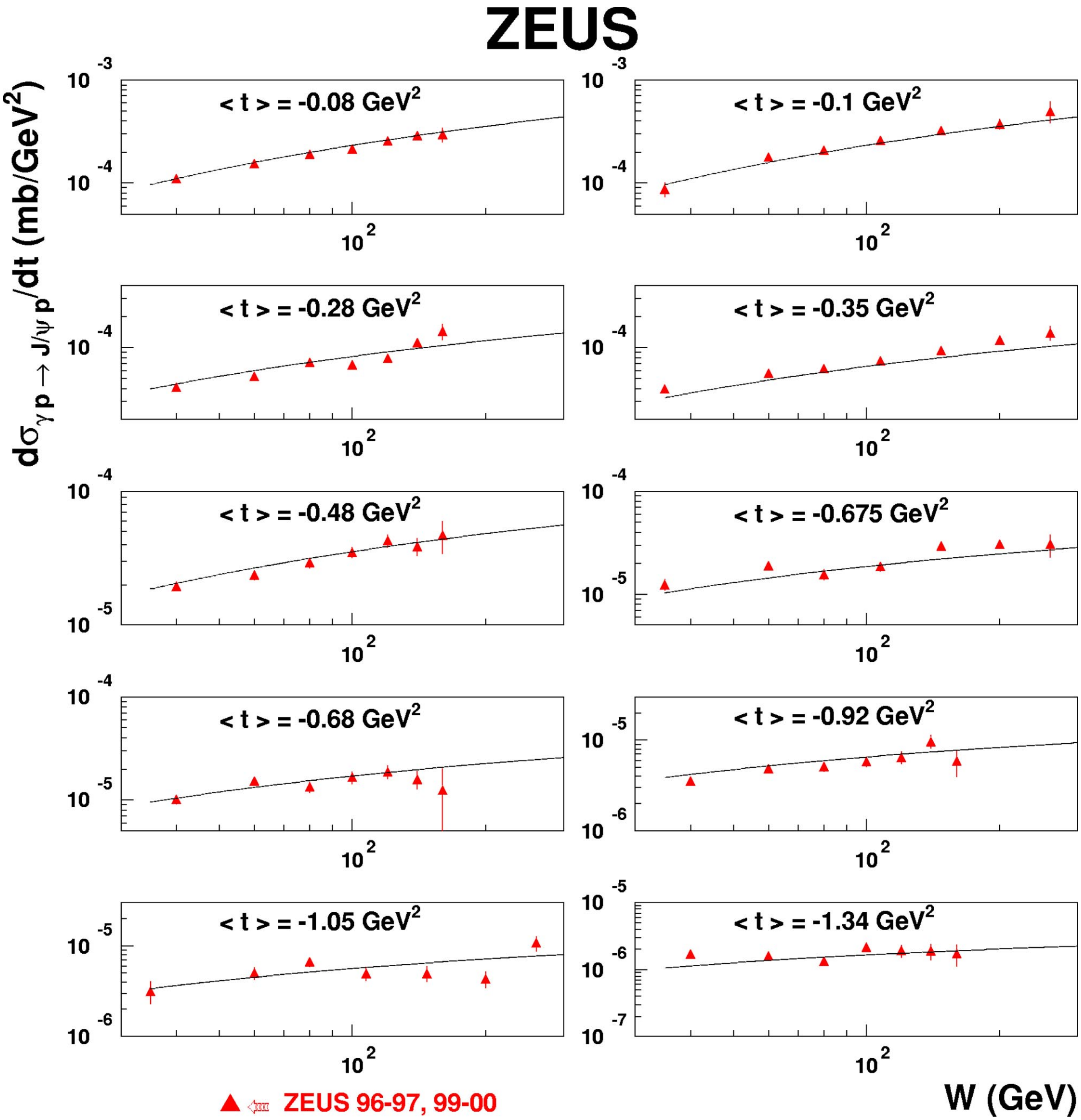

FIG. 5. (Color online) Differential cross section of exclusive J/ψ meson photoproduction as a function of W at different $\langle t\rangle$.

Choice II:

$$n=0.5, \quad \sigma_T(Q^2\to\infty)\sim\frac{1}{Q^6}; \tag{27}$$

Choice III:

$$n=0.25, \quad \sigma_T(Q^2\to\infty)\sim\frac{1}{Q^5}. \tag{28}$$

For the Reggeon couplings we have

$$f_{\mathbb{R}}(Q^2)=\left(\frac{c_1M_V^2}{c_1M_V^2+Q^2}\right)^{n_2}, \tag{29}$$

where c_1 is an adjustable parameter and $n_2=0.25,-0.25,-0.5$ for choices I, II, III.

Accordingly, in the case $Q^2\neq 0$ we use the following parametrizations for Reggeons couplings [compare with Eq. (21)]:

$$\hat{g}_{\mathbb{R}}(t;\tilde{Q}^2,M_V^2)=f_{\mathbb{R}}(Q^2)g_{\mathbb{R}}(t;\tilde{Q}^2,M_V^2). \tag{30}$$

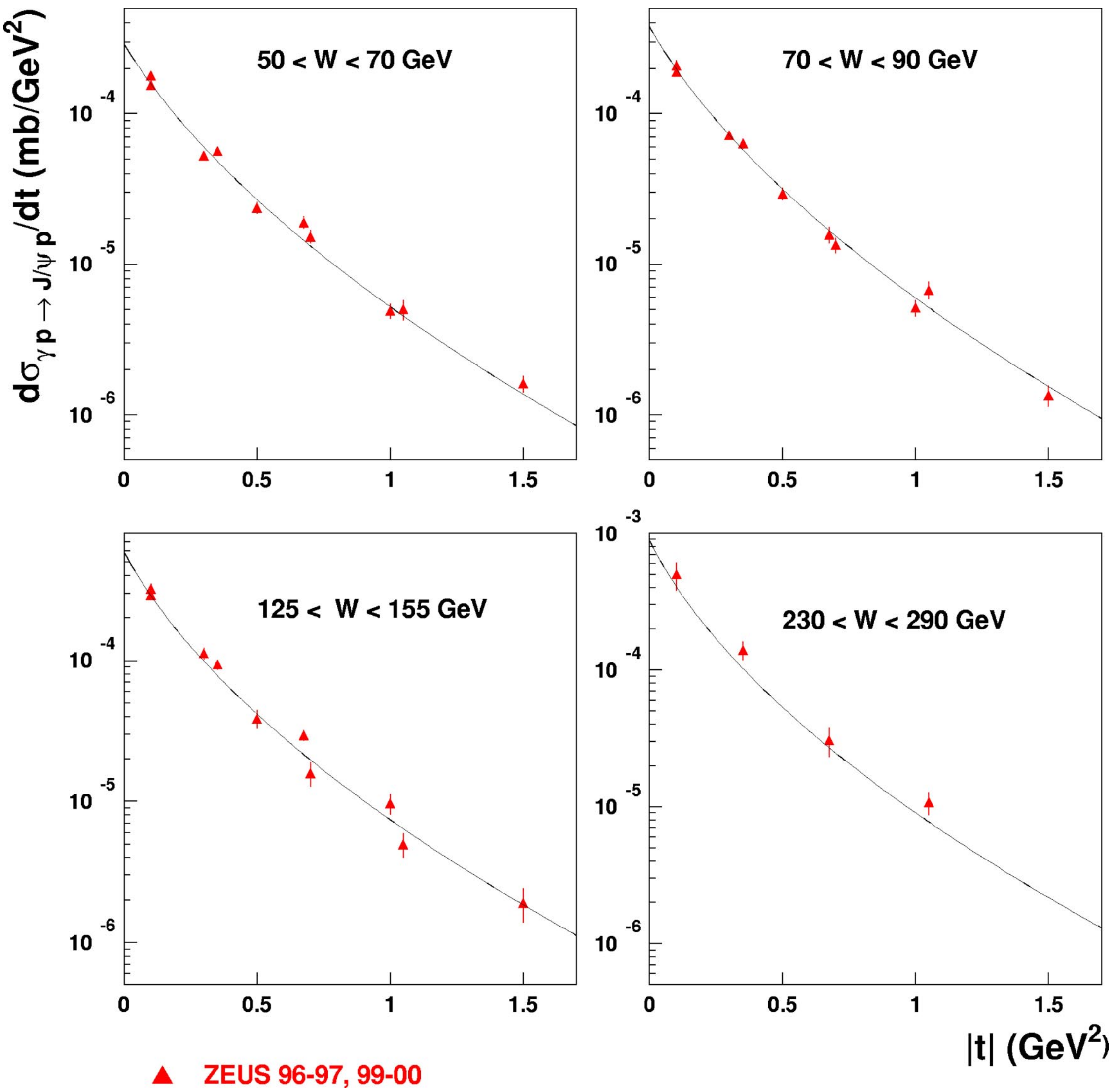

FIG. 6. (Color online) Differential cross section of exclusive J/ψ meson photoproduction.

The lack of data on the ratio σ_L/σ_T, especially in the high-Q^2 domain, does not allow us to draw definite conclusions about its asymptotic behavior (the Regge theory is not the appropriate tool for giving predictions in this case), nor do we have a unique prescription in the framework of our model. There may be several realizations of the model with different asymptotic behavior of σ_L/σ_T [2]. As a demonstration of such a possibility we explore the predictions (18) and use the following (most economical) parametrization for R (which cannot be deduced from the Regge theory) for choices I, II, III:

$$R(Q^2,M_V^2)=\left(\frac{cM_V^2+Q^2}{cM_V^2}\right)^{n_1}-1 \tag{31}$$

where c and n_1 are adjustable parameters for choices I, II, III.

We have, thus, three additional adjustable parameters as compared with real photoproduction. In order to obtain the values of the parameters for the case $Q^2\neq 0$, we fit just the data[3] on ρ_0 meson photoproduction in the region $0\leqslant Q^2 \leqslant 35$ GeV^2; the parameters for photoproduction by real photons are the same as in Table I. In order to avoid the low-W region where nucleon resonances may spoil the picture of ρ meson exclusive production, we restrict ourselves to the energy domain $W\geqslant 4$ GeV for $Q^2\neq 0$.

The parameters thus obtained are shown in Table II.

The results of the fit are depicted in Figs. 9–12. In these figures as well as in all the following ones the solid, dashed, and dotted lines correspond to the choices I, II, and III, respectively. The description of the data is very good at all energies. Both the high-energy data from ZEUS and H1 (Fig. 9) and the low-energy data from HERMES (Fig. 11) are accounted for. In the region of the HERMES data (Fig. 11)

[3]The data are available at REACTION DATA database http://durpdg.dur.ac.uk/hepdata/reac.html; CROSS SECTION PPDS database http://wwwppds.ihep.su:8001/c1-5A.html

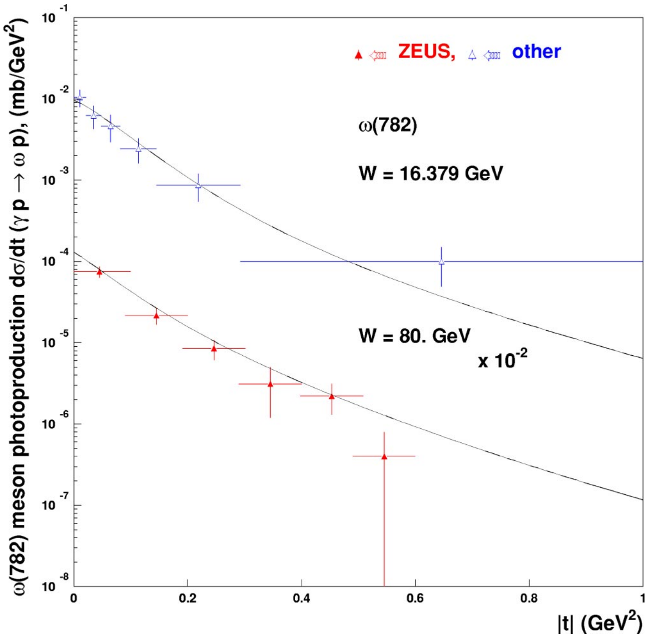

FIG. 7. (Color online) Differential cross section of exclusive ω meson photoproduction for $W=16.379$ and 80 GeV. The data and curves for $W=80$ GeV are scaled by a factor of 10^{-2}.

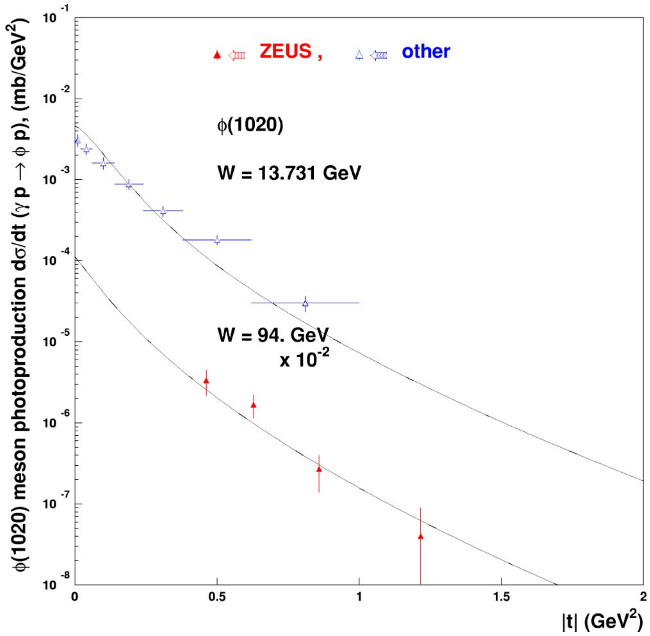

FIG. 8. (Color online) Differential cross section of exclusive φ meson photoproduction for $W=13.371$ and 94 GeV. The data and curves for $W=94$ GeV are scaled by a factor of 10^{-2}.

our description is comparable to that of Haakman, Kaidalov, and Koch [23] (see [24] for details).

We can now check the predictions of the model. As stated earlier, we aim at a unified model for all vector meson production, thus the only variable that changes is the mass of the vector meson. In Figs. 13–16 we depict our predictions for ω, φ, and J/ψ mesons and we compare them with the available data. The description of the data is very good for all the three mesons. The $\chi^2=0.89$ for J/ψ meson exclusive production follows without any fitting. Both W and Q^2 dependences are reproduced very well. Notice that, so far, the three choices I, II, and III all give equally acceptable reproduction of the data.

We now plot the various ratios σ_L/σ_T (these data were not fitted) corresponding to Eqs. (26),(27),(28) [shown with solid (choice I), dashed (choice II), and dotted (choice III) lines] in Figs. 17, 18, 19. The result shows, indeed, a rapid increase of σ_L/σ_T with increasing Q^2; however one can see that our intermediate choice II is preferable to either I or III on this basis.

Let us examine the dependences obtained. We find that the data prefer

$$R(Q^2\to\infty)\sim\left(\frac{Q^2}{M_V^2}\right)^{n_1}, \tag{32}$$

TABLE II. Parameters obtained by fitting ρ_0 virtual photoproduction data for choices I, II, III.

N	Parameter	Choice I	Choice II	Choice III
1	c	1.2666 ± 0.048	1.6900 ± 0.167	3.3282 ± 0.916
2	n_1	1.8355 ± 0.026	0.84596 ± 0.033	0.32453 ± 0.043
3	c_1	2.3258 ± 0.286	0.55469 ± 0.044	0.78464 ± 0.028
	Fit, No. of points		χ^2/DOF	
	$\rho_0(770)$, 283	1.47	1.53	1.56
	Meson, No. of points		χ^2 per point	
1	ρ_0, 283	1.45	1.51	1.54
2	ω, 67	1.46 (no fit)	1.46 (no fit)	1.46 (no fit)
3	φ, 56	0.78 (no fit)	0.79 (no fit)	0.82 (no fit)
2	J/ψ, 54	0.89 (no fit)	0.92 (no fit)	0.99 (no fit)

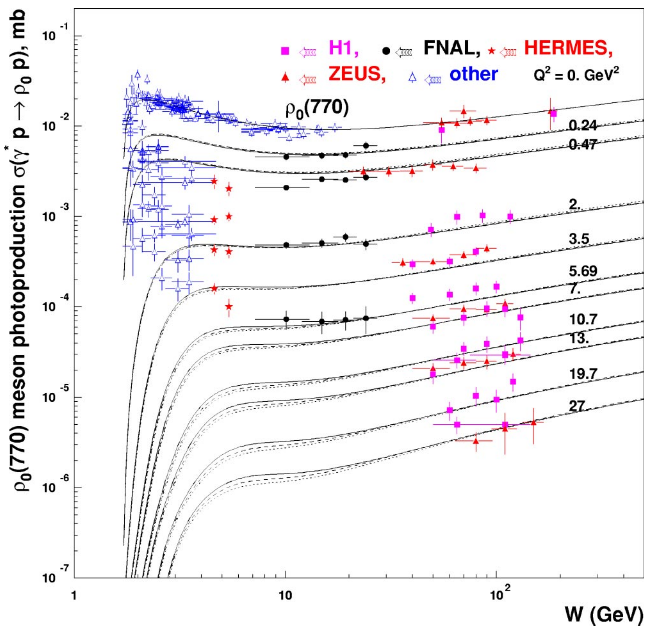

FIG. 9. (Color online) Elastic cross section of exclusive ρ_0 virtual photoproduction as a function of W for different values of Q^2.

where $n_1 \simeq 2$, 1, and 0.3 in choices I, II, and III. Our (probably oversimplified) estimates and the data show $0.3 < n_1 < 1$ (see Fig. 17); thus $\sigma \sim 1/Q^N$ where $N \in (4,4.4)$ as $N = 6 - 2n_1$ for choice II and $N = 5 - 2n_1$ for choice III. However, it is evident that new, more precise data on R are need.

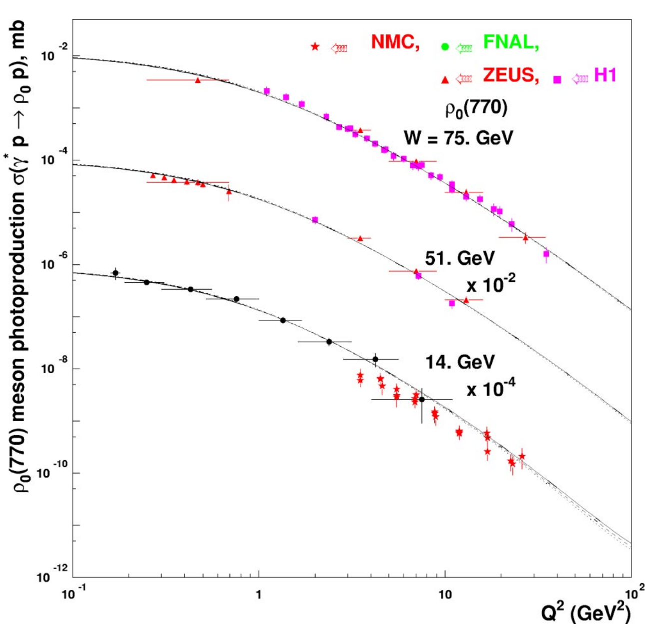

FIG. 10. (Color online) Elastic cross section of exclusive ρ_0 virtual photoproduction as a function of Q^2 for $W = 75$, 51, and 14 GeV. The data and curves for $W = 51$ and 14 GeV are scaled by the factors 10^{-2} and 10^{-4}.

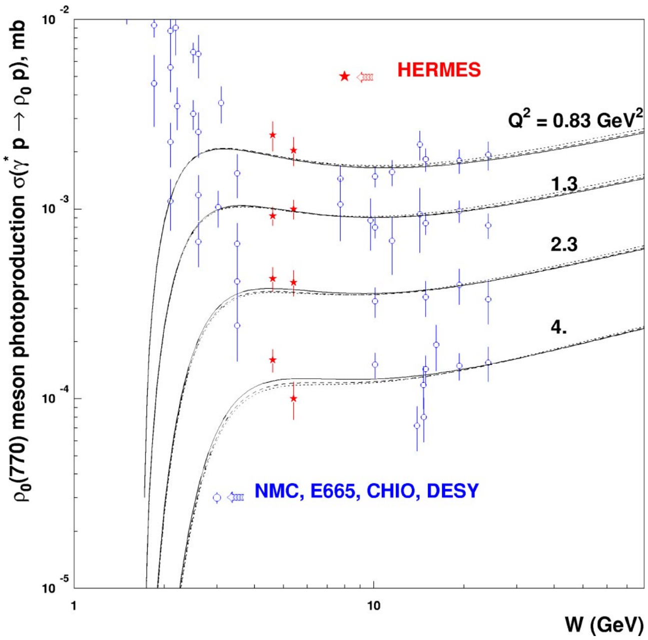

FIG. 11. (Color online) Elastic cross section of exclusive ρ_0 virtual photoproduction as a function of W for various Q^2 in the region of low and intermediate W.

III. CONCLUSION

We have shown that minor changes in the soft dipole Pomeron model recently developed [2] for vector meson photoproduction allow us to describe well the new ZEUS data [1] on the differential and integrated cross sections for $\gamma p \to J/\psi p$. Again, all available data on photoproduction of

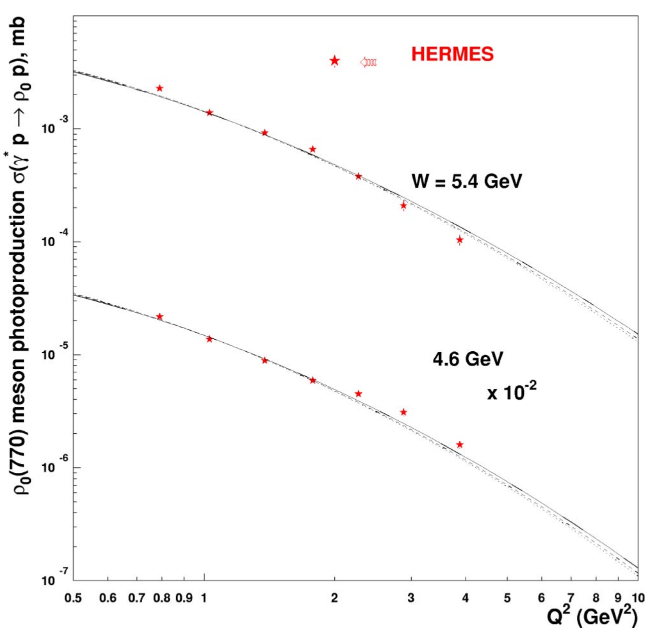

FIG. 12. (Color online) Elastic cross section of exclusive ρ_0 virtual photoproduction as a function of Q^2 for $W = 5.4$ and 4.6 GeV. The data and curves for $W = 4.6$ GeV are scaled by a factor of 10^{-2}.

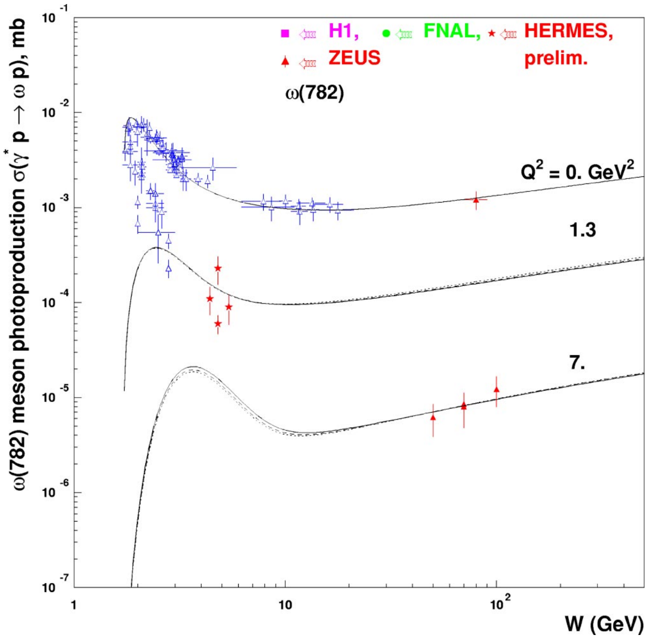

FIG. 13. (Color online) Elastic cross section of exclusive ω virtual photoproduction as a function of W for various Q^2.

other vector mesons at $Q^2=0$ as well as $Q^2\neq 0$ are well reproduced.

The changes made do not affect the main properties of the model, such as (i) the Pomeron intercept, which is equal to 1, and (ii) the hardness of the Pomeron, i.e., the fact that it is a double pole in the complex j plane.

We take the kinematical limits directly into account through the variable $z\propto\cos\theta_t$. The nonlinear Pomeron trajectory $\alpha_P(t)=1+\gamma(\sqrt{4m_\pi^2}-\sqrt{4m_\pi^2-t})$ turns out to be more suitable for the nonlinearity of the diffractive cone

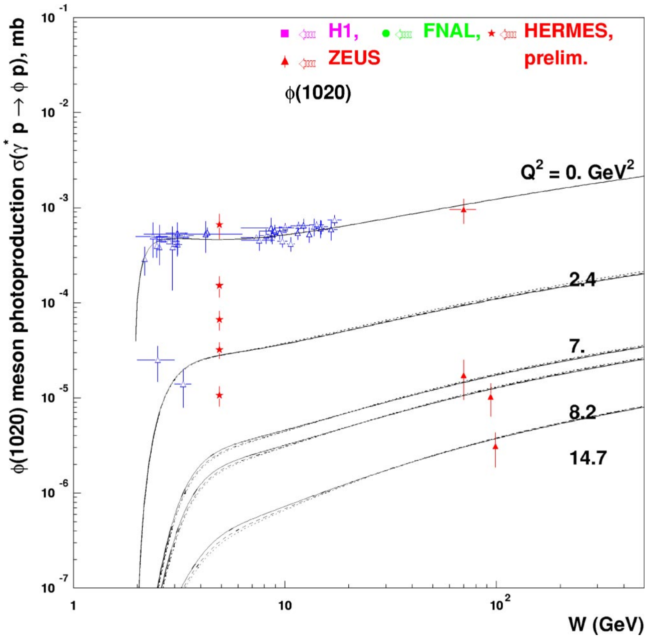

FIG. 14. (Color online) Elastic cross section of exclusive φ virtual photoproduction as a function of W for various Q^2.

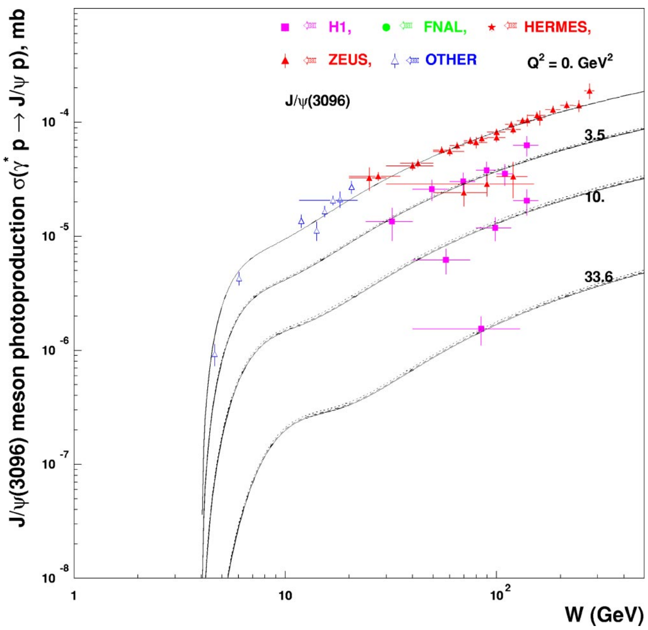

FIG. 15. (Color online) Elastic cross section of exclusive J/ψ virtual photoproduction as a function of W for various Q^2.

shown by the new ZEUS data. This is not unexpected as the linear behavior of the $\mathbb{P}$ trajectory is hard to reconcile with analyticity. We have also implemented the correct limits of t integration. The last circumstance allows us to account for the threshold behavior of the cross sections.

The present model does not pretend to be valid in the high-Q^2 region, although its interplay with perturbative QCD is extremely interesting, remaining however, due to the present state of the art at a rather speculative level. Consolidation of the two formalisms is still far from being completed (however, there are some attempts to investigate the problem; see, e.g., [25,26]).

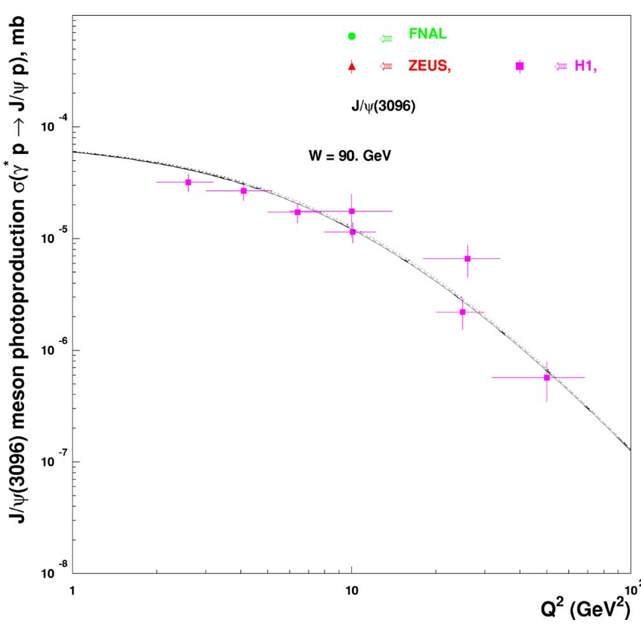

FIG. 16. (Color online) Elastic cross section of exclusive J/ψ virtual photoproduction as a function of Q^2 for $W=90$ GeV.

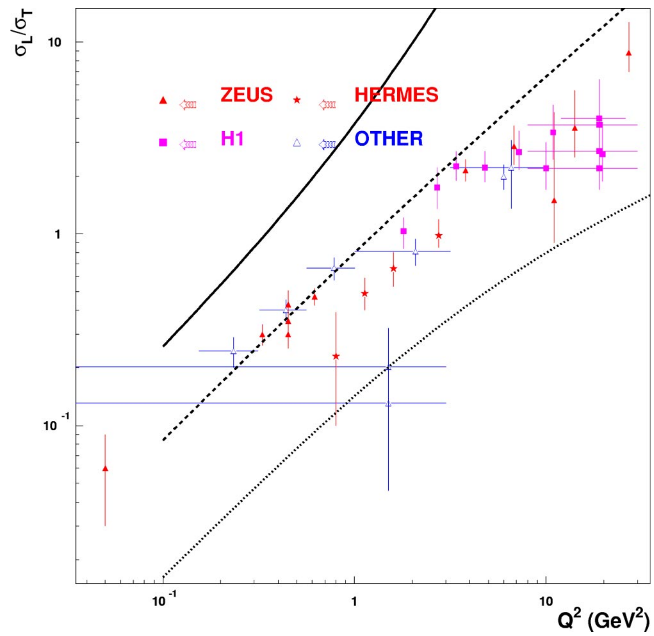

FIG. 17. (Color online) Ratio of σ_L/σ_T for exclusive ρ_0 large Q^2 photoproduction.

We would like to emphasize the following important points (confirming the main findings of [2] and repeating some of them).

(1) The new ZEUS data [1] (in contrast to the old ones) quite definitely point toward nonlinearity of the Pomeron slope and trajectory.

(2) Our model describes the data also at low energies due to the kinematical shrinkage of the available t region. This is particularly important for J/ψ production where the bulk of the available data are not so far from its threshold.

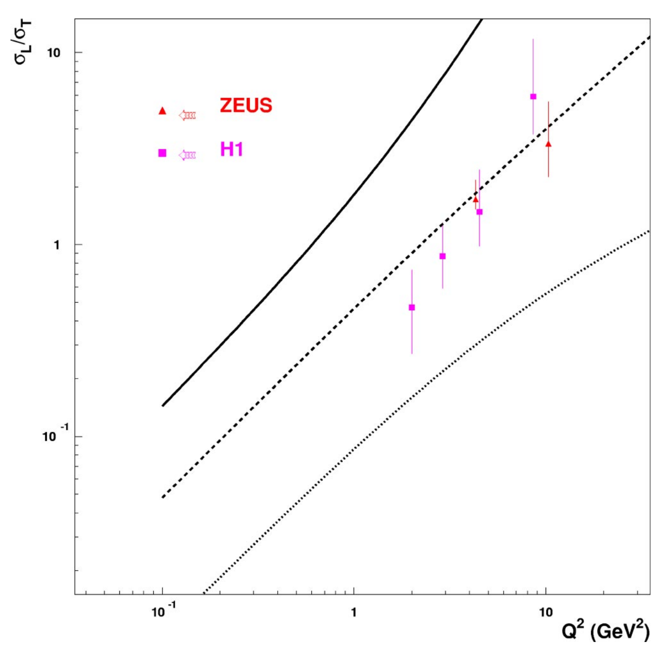

FIG. 18. (Color online) Ratio of σ_L/σ_T for exclusive φ large Q^2 photoproduction.

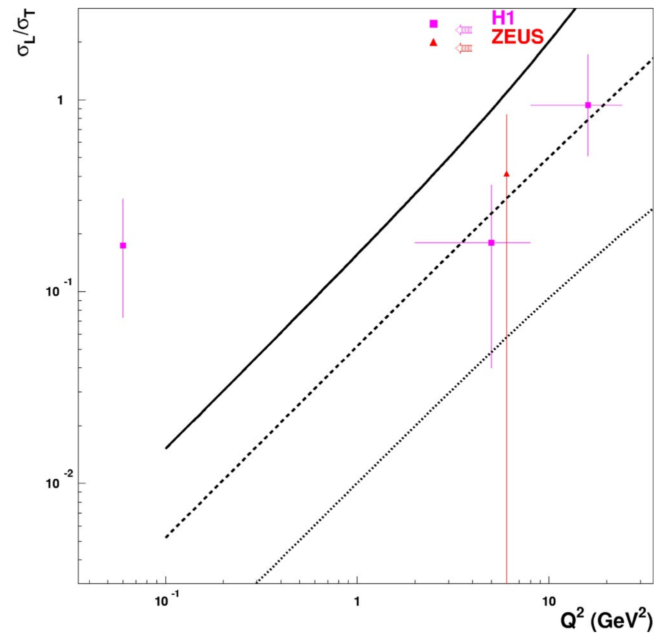

FIG. 19. (Color online) Ratio of σ_L/σ_T for exclusive J/ψ large Q^2 photoproduction.

(3) Phenomenologically, we find that in the region of available Q^2 the ratio $\sigma_L/\sigma_T \sim (Q^2/M_V^2)^{n_1}$, where $0.3 < n_1 < 1$. The definite conclusion can be derived only with new precise data on the ratio σ_L/σ_T, especially for high Q^2.

(4) Pomeron and secondary Reggeons appear as universal objects in Regge theory [7]. The corresponding j singularities of the γp amplitudes are universal. They do not depend on the properties of the external particles and, consequently, on Q^2 (only residues or vertex functions may depend on Q^2). We believe that the unitarity restrictions on the Pomeron contribution obtained strictly for the hh case must hold also for γh if it is universal.

(5) The growth with energy of hadronic total cross sections and the restriction on the Pomeron intercept [$\alpha_{\mathbb{P}}(0) \leq 1$] implied by the Froissart-Martin bound [14] imply that the Pomeron is a more complicated singularity than a simple pole with $\alpha_{\mathbb{P}}(0)=1$. We have considered the simplest case when the Pomeron is a double j pole leading to $\sigma(s) \propto \ln s$. We have shown that one does not need a contribution with $\alpha(0)>1$ (hard Pomeron) violating unitarity in order to describe the exclusive photoproduction data in the present region of Q^2 and t.

(6) The model predicts two effects that would be observed at high energies: a flattening of the J/ψ integrated cross section and a rise of the φ cross section faster than the ω one.

ACKNOWLEDGMENTS

We would like to thank Michele Arneodo, Alexei Kaidalov, Alexander Borissov, Jean-Rene Cudell, and Alessia Bruni for various and fruitful discussions. One of us (E.M.) would like to thank the Department of Theoretical Physics of the University of Torino for its hospitality and financial support during his visit to Turin.

[1] ZEUS Collaboration, S. Chekanov *et al.*, Eur. Phys. J. C **24**, 345 (2002).
[2] E. Martynov, A. Prokudin, and E. Predazzi, Eur. Phys. J. C **26**, 271 (2002).
[3] V. N. Gribov, B. L. Ioffe, and I. Ya. Pomeranchuk, Yad. Fiz. **2**, 768 (1965); B. L. Ioffe, Phys. Lett. **30B**, 123 (1968).
[4] S. J. Brodsky, L. Frankfurt, J. F. Gunion, A. H. Mueller, and M. Strikman, Phys. Rev. D **50**, 3134 (1994).
[5] J. R. Cudell, A. Donnachie, and P. V. Landshoff, Phys. Lett. B **448**, 281 (1999).
[6] P. Desgrolard and E. Martynov, Eur. Phys. J. C **22**, 479 (2001).
[7] For a recent update on the Regge theory, see, V. Barone and E. Predazzi, *High-Energy Particle Diffraction* (Springer-Verlag, Berlin, 2002).
[8] J. J. Sakurai, Ann. Phys. (N.Y.) **11**, 1 (1960); M. Gell-Mann and F. Zachariasen, Phys. Rev. **124**, 953 (1961).
[9] Particle Data Group, D. E. Groom *et al.*, Eur. Phys. J. C **15**, 1 (2000).
[10] J. Nemchik, N. N. Nikolaev, E. Predazzi, and B. G. Zakharov, Z. Phys. C **75**, 71 (1997).
[11] P. Desgrolard, M. Giffon, A. Lengyel, and E. S. Martynov, Nuovo Cimento Soc. Ital. Fis., A **107**, 637 (1994).
[12] COMPETE Collaboration, J. R. Cudell *et al.*, Phys. Rev. D **65**, 074024 (2002).
[13] E. S. Martynov, ''Unitarization of Pomeron and Regge Phenomenology of Deep Inelastic Scattering,'' in Proceedings of the Workshop ''Hadrons-94,'' Kiev, 1994, Report No. ITP-94-49E, Kiev, 1994; L. Jenkovszky, E. Martynov, and F. Paccanoni, ''Regge Behavior of the Nucleon Structure Function,'' Padova Report No. DFPD 95/TH/21, 1995.
[14] M. Froissart, Phys. Rev. **123**, 1053 (1961); A. Martin, *ibid.* **129**, 993 (1963).
[15] A. Donnachie and P. V. Landshoff, Phys. Lett. B **185**, 403 (1987); **348**, 213 (1995).
[16] L. Fonda and R. G. Newton, Nuovo Cimento **14**, 1027 (1959).
[17] L. L. Jenkovszky, E. S. Martynov, and F. Paccanoni, ''Regge Pole Model for Vector Meson Photoproduction at HERA,'' hep-ph/9608384.
[18] R. Fiore, L. L. Jenkovszky, and F. Paccanoni, Eur. Phys. J. C **10**, 461 (1999); R. Fiore, L. L. Jenkovszky, F. Paccanoni, and A. Papa, Phys. Rev. D **65**, 077505 (2002).
[19] E. Predazzi, Ann. Phys. (N.Y.) **36**, 250 (1966).
[20] H1 Collaboration, C. Adloff *et al.*, Phys. Lett. B **483**, 23 (2000).
[21] J. R. Cudell and I. Royen, Phys. Lett. B **397**, 317 (1997).
[22] J. R. Cudell and I. Royen, Nucl. Phys. **B545**, 505 (1999).
[23] L. P. A. Haakman, A. Kaidalov, and J. H. Koch, Phys. Lett. B **365**, 411 (1996).
[24] HERMES Collaboration, A. Airapetian *et al.*, Eur. Phys. J. C **17**, 389 (2000).
[25] G. Soyez, hep-ph/0211361.
[26] A. Donnachie and P. V. Landshoff, Phys. Lett. B **533**, 277 (2002); Cudell, Donnachie, and Landshoff [5].